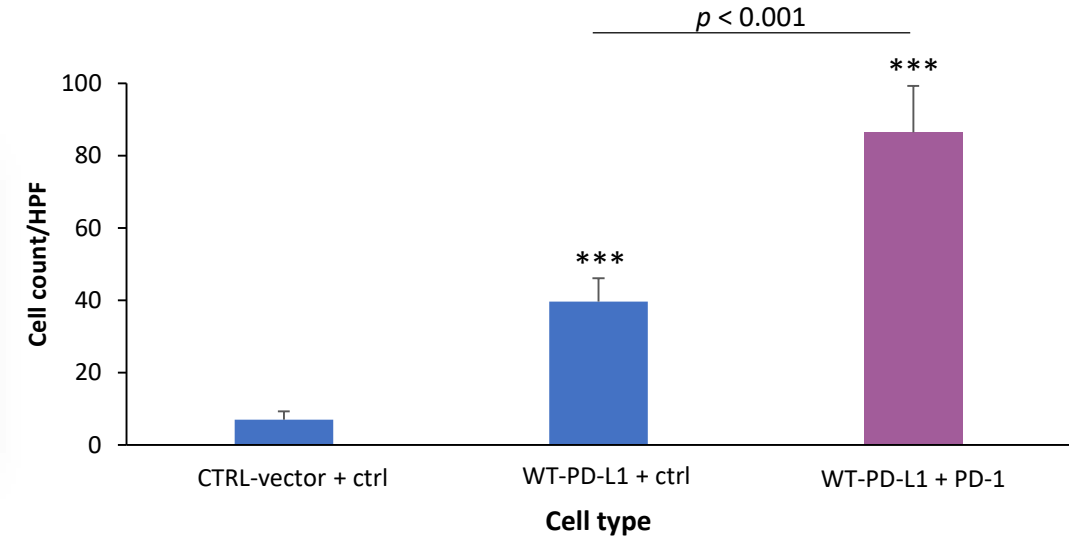
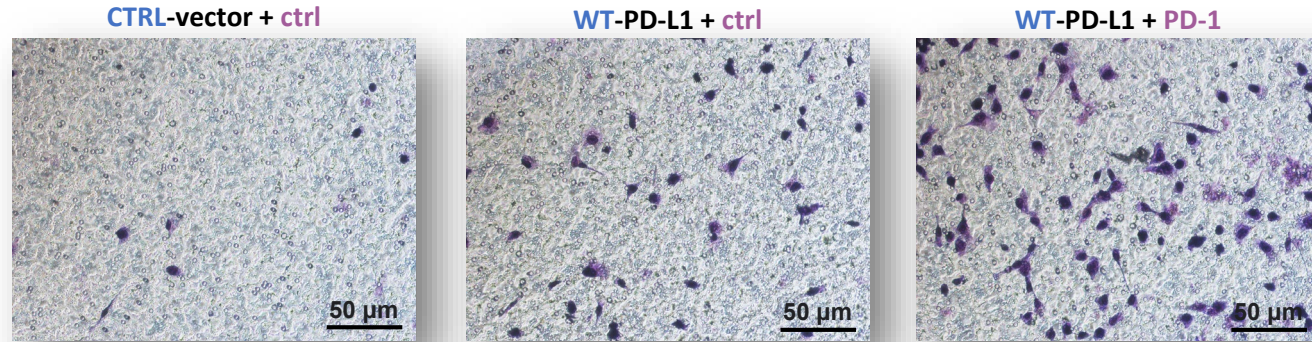
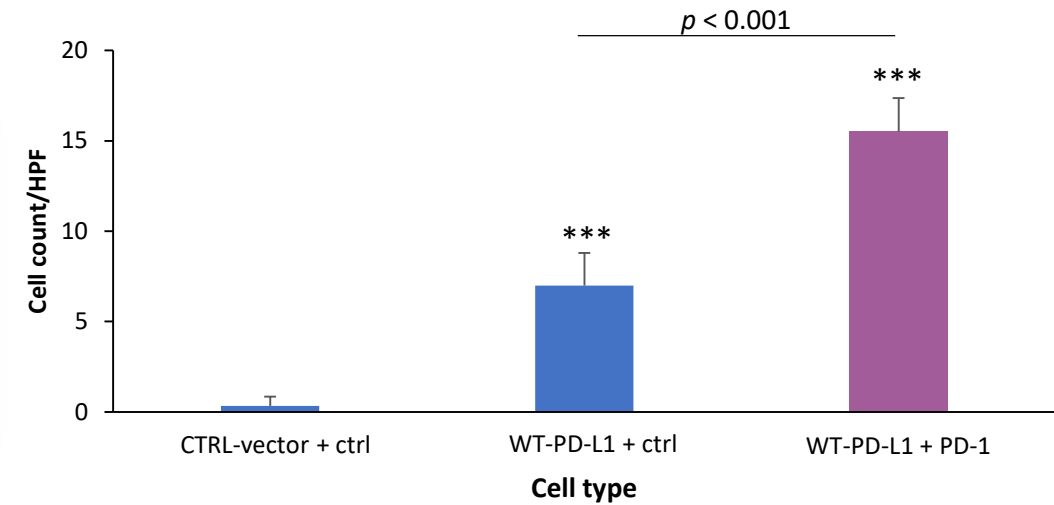
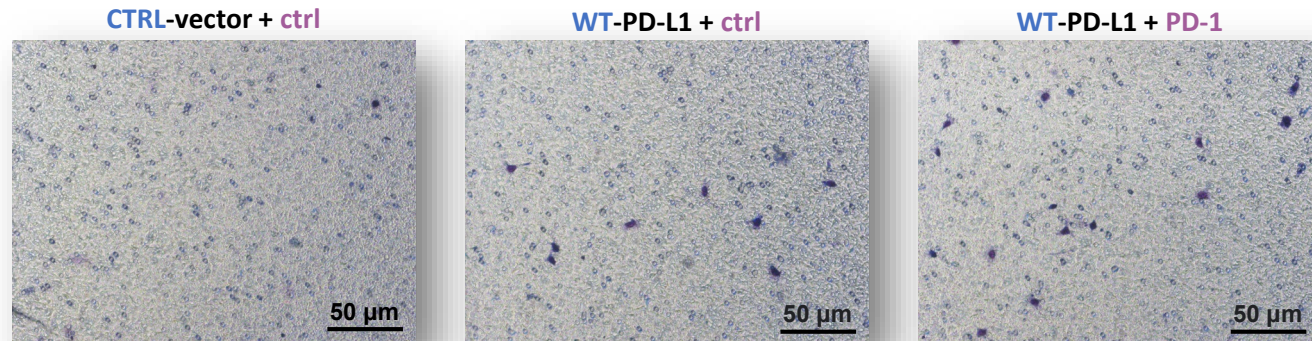


Fig. S1

A. BT + PD-1:
Invasion through lung ECM



B. MCF-7 + PD-1:
Invasion through bone ECM

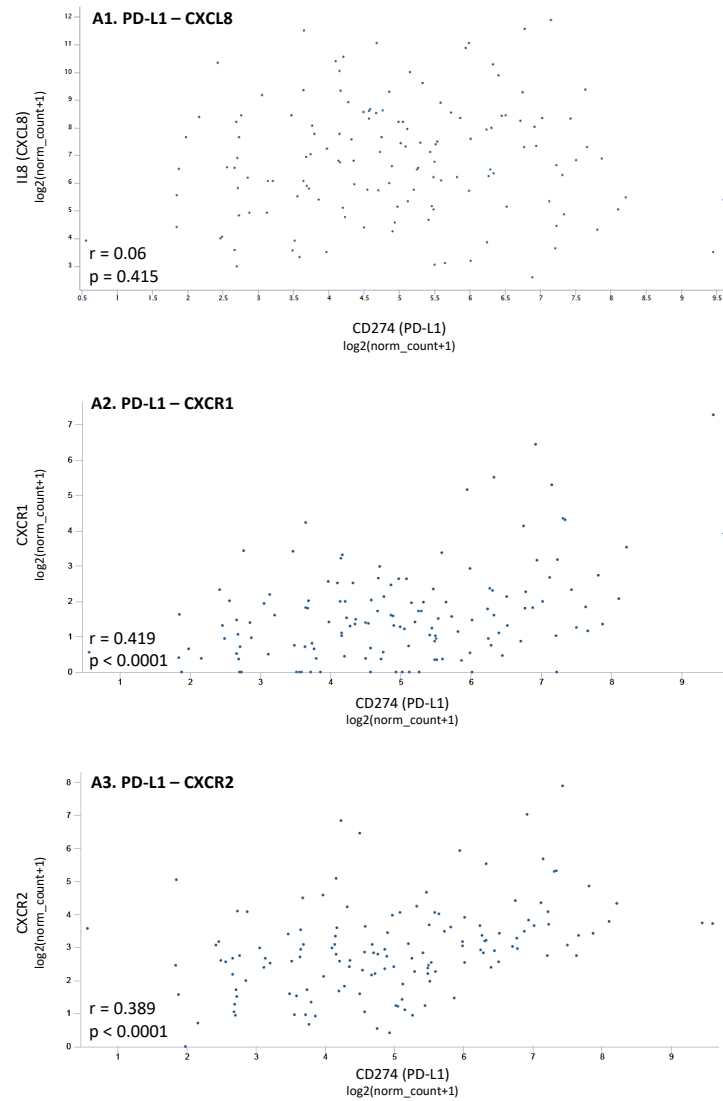


Autonomous activities of PD-L1 increase tumor cell invasion through ECM substrates, and these activities are further potentiated by exposure to PD-1

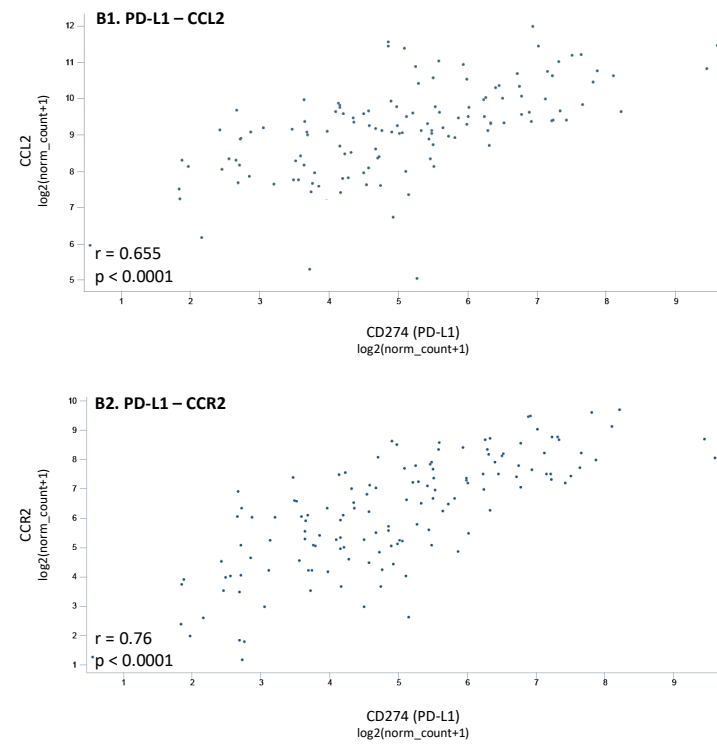
Invasion of (A) WT-PD-L1-BT cells and (B) WT-PD-L1-MCF-7 cells was determined in ECM-coated transwells. WT-PD-L1-over-expressing cells and CTRL-vector cells were cultured and 24 hrs later, PD-1 or its control (ctrl), were added at 2μg/ml for 72 hrs. Tumor cell invasion was performed under the following conditions: BT cells: Lung ECM, for 30 hrs; MCF-7 cells: Bone ECM, for 54 hrs. Each panel demonstrates the results of a representative experiment out of n=3. ***p<0.001.

Fig. S2

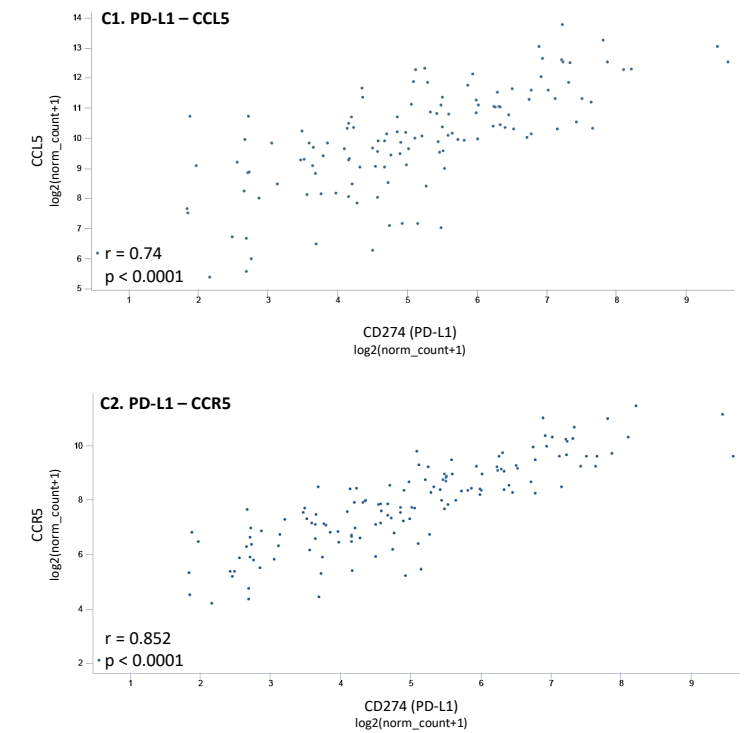
A. Correlation: PD-L1 with the CXCL8 – CXCR1/2 axis



B. Correlation: PD-L1 with the CCL2 – CCR2 axis



C. Correlation: PD-L1 with the CCL5 – CCR5 axis

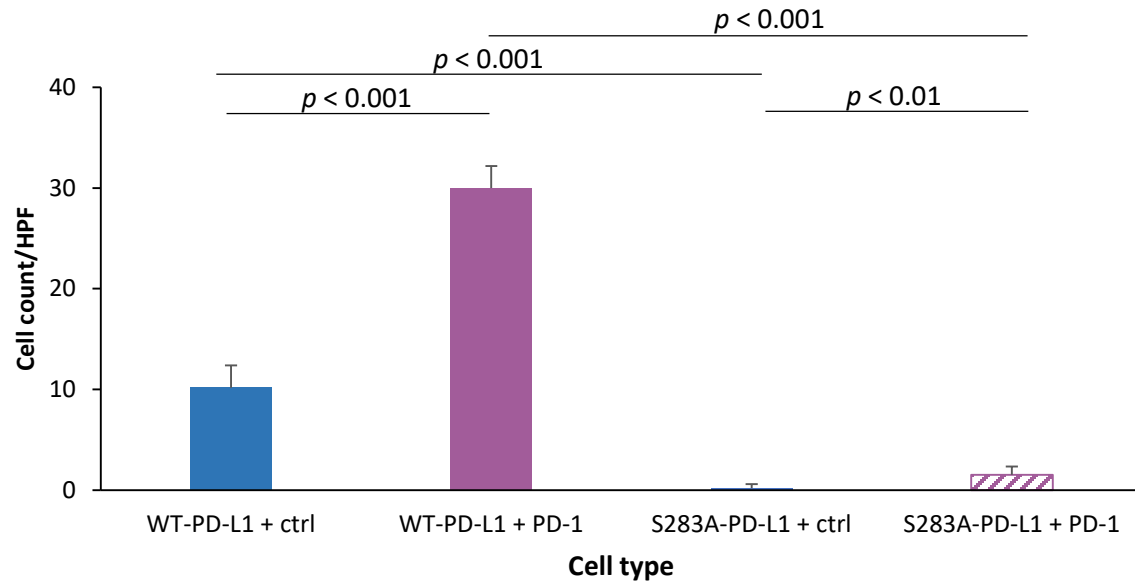


PD-L1 expression is highly correlated with the CCL2 - CCR2 and the CCL5 - CCR5 axes in basal breast cancer patients

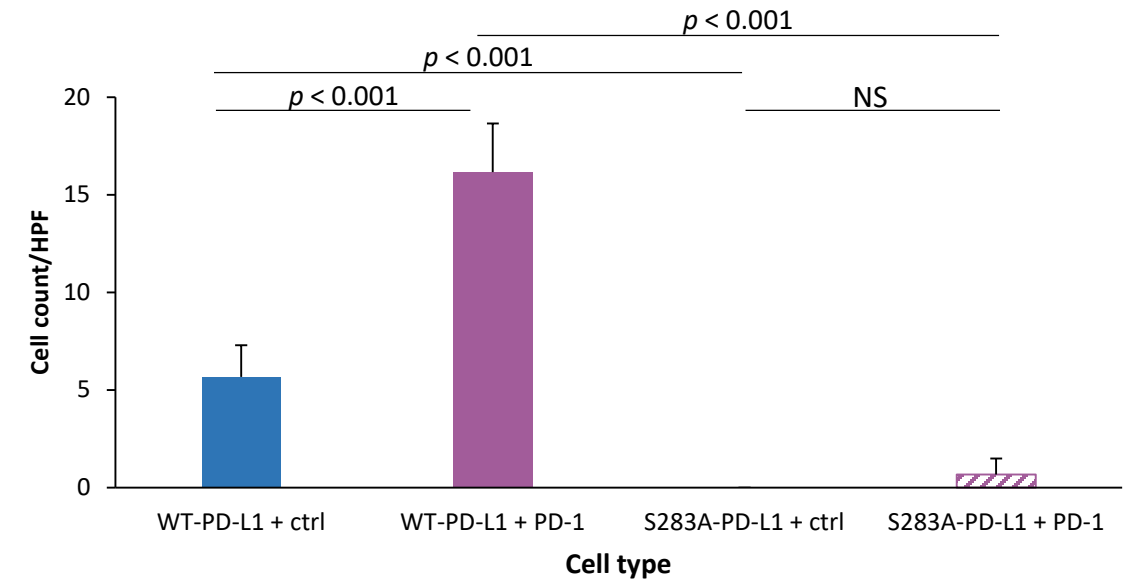
Data available in the TCGA dataset was used to identify correlations in gene expression in basal patients. n=141. **(A)** Correlations of PD-L1 with members of the CXCL8 – CXCR1/2 axis. (A1) CXCL8, (A2) CXCR1, (A3) CXCR2. **(B)** Correlations of PD-L1 with members of the CCL2 – CCR2 axis. (B1) CCL2, (B2) CCR2. **(C)** Correlations of PD-L1 with members of the CCL5 – CCR5 axis with PD-L1. (C1) CCL5, (C2) CCR5.

Fig. S3

A. MDA: S283A-PD-L1 + PD-1 - Invasion through lung ECM



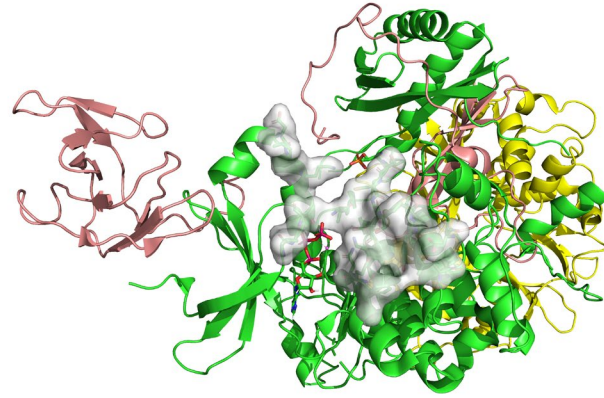
B. MCF-7: S283A-PD-L1 + PD-1 - Invasion through bone ECM



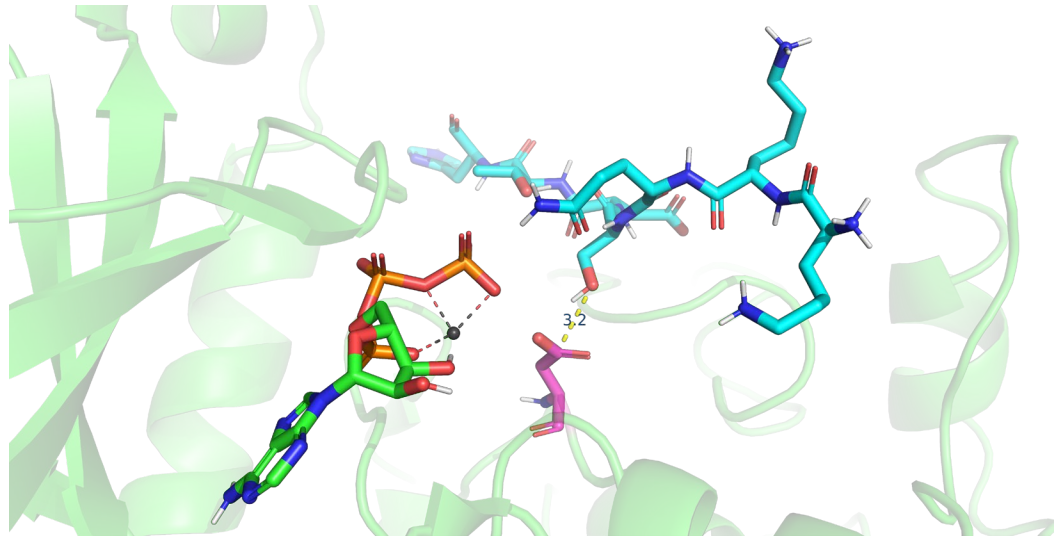
Invasion through ECM substrates - via cell-autonomous and PD-1-induced activities of PD-L1 - are fully dependent on S283 integrity

Invasion of (A) MDA cells and (B) MCF-7 cells that over-expressed WT-PD-L1 or S283A-PD-L1 was determined in transwell assays, after exposure to PD-1 or its control (ctrl). Cell invasion was determined in ECM-coated transwells for the time points indicated in Figure S1: lung ECM in the case of MDA cells and bone ECM in the case of MCF-7 cells. PD-1 or its control ctrl were added one day after culturing, at 2µg/ml, for 72 hrs. Each panel demonstrates the results of a representative experiment out of n=3. p values are demonstrated in the Figure. NS, Non-significant.

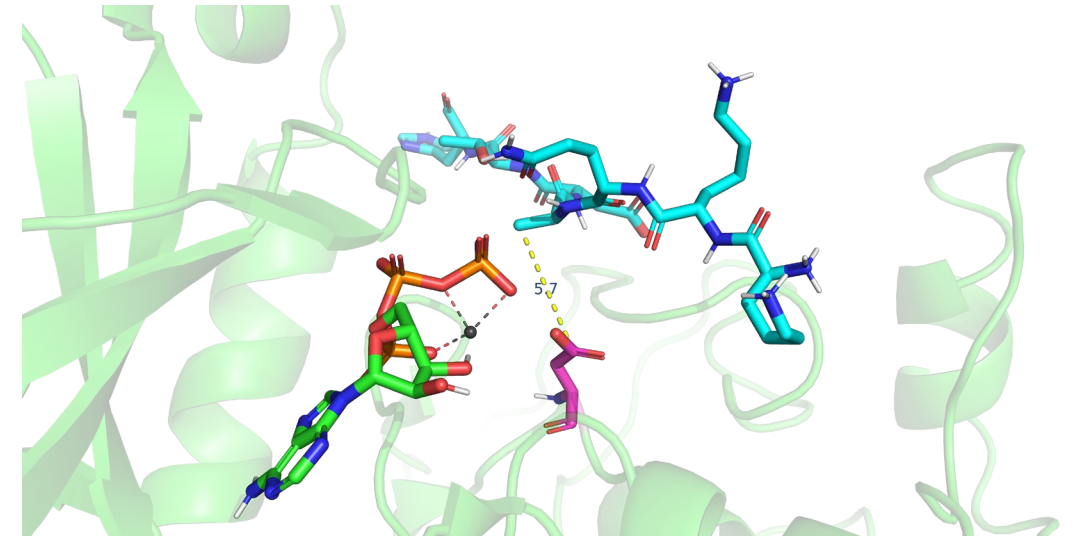
A. AMPK structure



B1. AMPK – S283 (in WT-PD-L1)



B2. AMPK – A283 (in S283A-PD-L1)

**Modeling of AMPK binding to peptides containing S283 and S283A**

(A) The structure of AMPK, determined by PDB ID 4RER. Green, the catalytic α subunit of AMPK. White, surface residues that make contacts with substrates. Burgundy, the β subunit of AMPK. Yellow, the γ subunit of AMPK. **(B)** Modeling of the 7-aa peptide complexes that contain either the native S283 residue that is expressed in WT-PD-L1 (B1) or the A283 residue of mutated S283A-PD-L1 (B2), in AMPK catalytic site. Figures were generated by PyMol. Non polar hydrogens are not demonstrated. Green, carbons in AMPK. Magenta, catalytic aspartate. Cyan, 7-aa peptides. In B1, the dashed line demonstrates the distance between carbon in aspartate and hydrogen in serine. In B2, due to the lack of hydrogen in alanine, the dashed line demonstrates the distance between the carbon in aspartate and carbon in alanine.

Table S1

MMGBSA_dG_Bind										
Title	total	Coulomb	Covalent	Hbond	Lipo	Packing	SelfCont	Solv_GB	Solv_SA	vdW
Native	-26.75	-17.96	0.04	-3.80	-4.19	0.00	0.00	41.34		-42.18
Mutant	-2.48	-25.24	2.35	-2.13	-5.68	0.00	0.00	77.17		-48.94
Lig_Strain										
Title	total	Coulomb	Covalent	Hbond	Lipo	Packing	SelfCont	Solv_GB	Solv_SA	vdW
Native	11.85	30.40	0.51	2.43	0.02	0.00	0.00	-23.82		2.30
Mutant	12.58	11.00	2.82	0.04	-0.11	0.00	0.00	-3.84		2.66
Ligand										
Title	total	Coulomb	Covalent	Hbond	Lipo	Packing	SelfCont	Solv_GB	Solv_SA	vdW
Native	-242.61	-193.27	33.38	-3.50	-1.98	0.00	0.00	-88.56		11.31
Mutant	-238.04	-163.98	27.32	-1.54	-1.87	0.00	0.00	-110.91		12.94
Complex										
Title	total	Coulomb	Covalent	Hbond	Lipo	Packing	SelfCont	Solv_GB	Solv_SA	vdW
Native	-11394.59	-8251.71	1185.92	-147.01	-606.27	-23.45	-13.31	-2262.25		-1276.51
Mutant	-11370.35	-8230.92	1179.50	-143.57	-607.68	-23.44	-13.31	-2248.63		-1282.29
Receptor										
Title	total	Coulomb	Covalent	Hbond	Lipo	Packing	SelfCont	Solv_GB	Solv_SA	vdW
Native	-11125.23	-8040.48	1152.51	-139.71	-600.10	-23.45	-13.31	-2215.03		-1245.65
Mutant	-11129.83	-8041.70	1149.83	-139.90	-600.14	-23.44	-13.31	-2214.88		-1246.29
MMGBSA_dG_Bind(NS)										
Title	total	Coulomb	Covalent	Hbond	Lipo	Packing	SelfCont	Solv_GB	Solv_SA	vdW
Native	-38.60	-48.37	-0.48	-6.23	-4.21	0.00	0.00	65.16		-44.48
Mutant	-15.06	-36.25	-0.47	-2.17	-5.57	0.00	0.00	81.00		-51.61
Rec_Strain										
Title	Energy	Coulomb	Covalent	Hbond	Lipo	Packing	SelfCont	Solv_GB	Solv_SA	vdW
Native	0.00	0.00	0.00	0.00	0.00	0.00	0.00	0.00		0.00
Mutant	0.00	0.00	0.00	0.00	0.00	0.00	0.00	0.00		0.00
Prime_MMGBSA_ligand										
Title	efficiency	efficiency_sa	efficiency_ln							
Native	-0.46	-0.69	-5.29							
Mutant	-0.04	-0.07	-0.49							

MMGBSA calculations of binding efficiency of WT-PD-L1-derived peptide and S283A-PD-L1-derived peptide to AMPK

The Table demonstrates MMGBSA calculations of relevant parameters. Native: S283-containing WT-PD-L1-derived peptide; Mutant: S283A-PD-L1-derived peptide.